

η in the nuclear medium within a chiral unitary approach

T. Inoue* and E. Oset

Departamento de Física Teórica and IFIC, Centro Mixto Universidad de Valencia-CSIC
Institutos de Investigación de Paterna, Apdo. correos 22085, 46071, Valencia, Spain

Abstract

The self-energy of an η meson in the nuclear medium is calculated in a chiral unitary approach. A coupled channel Bethe-Salpeter equation is solved to obtain the effective η - N interaction in the medium. The base model reproduces well the free space π - N elastic and inelastic scattering at the η - N threshold or $N^*(1535)$ region. The Pauli blocking on the nucleons, binding potentials for the baryons and self-energies of the mesons are incorporated, including the η self-energy in a self-consistent way. Our calculation predicts about $-54 - i29$ MeV for the optical potential at normal nuclear matter for an η at threshold but also shows a strong energy dependence of the potential.

1 Introduction

The nuclear medium effects on meson properties are interesting and have been investigated extensively. The data from relativistic heavy ion collision at CERN [1, 2, 3] and at lower energies at Bevalac [4, 5], may indicate either a lowering of the ρ meson mass or a large broadening of its width. In the near future, experiments at GSI(HADES collaboration [6, 7]) could clarify the situation by providing better statistics and mass resolution. The recent discovery of the deeply bound state of π^- in Pb [8, 9] reveals an upward shift of the pion mass of about 20 MeV, and confirms the repulsive S-wave interaction of the π^- in nuclear matter already established from studies of the bulk pionic atom data [10, 11, 12]. The low energy magnitudes of the η - N interaction and the properties of the η meson in the medium, are still open questions. The η mesic nuclei are expected to provide such informations and are searched at several facilities. For example, the ${}^7\text{Li}(d, {}^3\text{He})_{\eta}{}^6\text{He}$, ${}^{12}\text{C}(d, {}^3\text{He})_{\eta}{}^{11}\text{B}$ and ${}^{27}\text{Al}(d, {}^3\text{He})_{\eta}{}^{26}\text{Mg}$ reactions are investigated at GSI [13].

In this paper, we study the properties of the η in the medium from a theoretical point of view. We evaluate the effective S-wave η - N interaction in the medium in a chiral unitary approach. The self-energy of η is obtained by summing the ηN interaction in the medium over the nucleons in the Fermi sea. The present work follows closely the method used in [14] to evaluate the \bar{K} nucleus optical potential in a self-consistent way. In the next section, we explain our approach. We show our input related with the nuclear medium in section 3. The results are given in section 4. Section 5 is devoted to the conclusions.

*e-mail: inoue@ific.uv.es

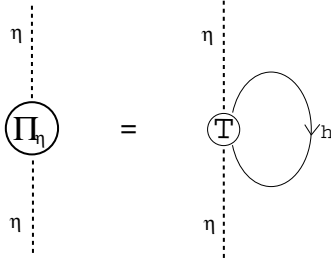


Figure 1: Diagrammatic representation of the η self-energy from S-wave interaction with nucleons.

2 Chiral unitary approach to the η self-energy

We want to obtain the self-energy of the η meson in nuclear matter at various densities ρ , as a function of the η energy k^0 and the momentum \vec{k} in the nuclear matter frame. In this paper, we calculate it by means of

$$\Pi_\eta(k^0, \vec{k}; \rho) = 2 \int^{k_F} \frac{d^3 \vec{p}_n}{(2\pi)^3} T_{\eta n}(P^0, \vec{P}; \rho) \times 2 \quad (1)$$

where \vec{p}_n and k_F are the momentum of the neutron and the Fermi momentum at density ρ respectively, and $T_{\eta n}(P^0, \vec{P}; \rho)$ is the η -neutron in-medium S-wave interaction, with the total 4-momentum of the system (P^0, \vec{P}) in the nuclear matter frame, namely $P^0 = k^0 + E_n(\vec{p}_n)$ and $\vec{P} = \vec{k} + \vec{p}_n$. Here, the isospin symmetry, $T_{\eta p} = T_{\eta n}$, is assumed and the amplitude is summed over nucleons in the Fermi sea as shown in Fig.1. We shall be concerned about the S-wave η self-energy. At low energies of the η this part of the potential is largely dominant.

We evaluate the in-medium amplitude $T_{\eta n}$ in a chiral unitary approach. For this purpose we follow the model for the free space π - N and coupled channels scattering of ref.[15], which reproduces the experimental data of πN scattering up to energies above the $N^*(1535)$ region. A similar chiral approach which covers a wider energy range in isospin 1/2, although with more free parameters, is also done in ref.[16].

In ref.[15] the Bethe-Salpeter equation is considered with eight coupled channels including two $\pi\pi N$ states, namely $\{\pi^- p, \pi^0 n, \eta n, K^0 \Lambda, K^+ \Sigma^-, K^0 \Sigma^0, \pi^0 \pi^- p, \pi^+ \pi^- n\}$. The kernels for the meson-baryon two-body sector are taken from the lowest order chiral Lagrangians and improved by applying a form factor corresponding to a vector meson exchange in the t-channel. The kernels for $\pi N \leftrightarrow \pi\pi N$ transitions are determined so that they account for both the πN elastic and $\pi N \rightarrow \pi\pi N$ processes. That model reproduces well the πN scattering amplitudes, especially in isospin 1/2, for the center of mass energy energies from threshold to 1600 MeV. It reproduce also the $\pi^- p \rightarrow \eta n$ cross section at the region where the P-wave contribution is negligible. In this coupled channels approach, the model also provides the η - n interaction in free space and generates dynamically the $N^*(1535)$ resonance providing the width and branching ratios for its decay in good agreement with experiment, among them the ηN branching ratio which is quite large for that resonance. The agreement of the model with the different available data around $N^*(1535)$ resonance region and the adequate description of the properties of the resonance, in particular the strong coupling to the ηN state, give us confidence that the model is rather accurate to make predictions on the $\eta N \rightarrow \eta N$ interaction. Therefore we use this model as a base to take nuclear matter effects into account.

Analogously to the free space case, $T_{\eta n}(P^0, \vec{P}; \rho)$ is given by one matrix element of the matrix

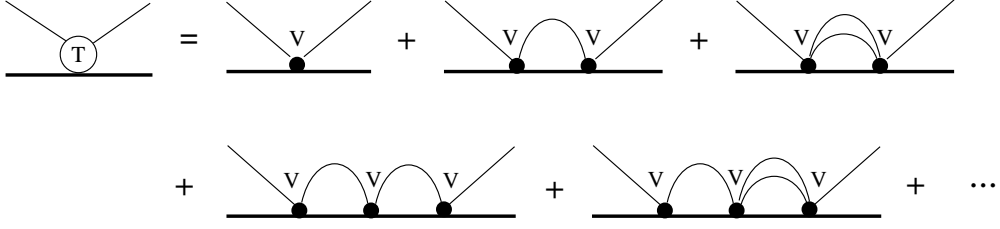


Figure 2: Diagrammatic representation of the Bethe-Salpeter equation.

equation in the space of coupled channels

$$T(P^0, \vec{P}; \rho) = [1 - V(\sqrt{s})G(P^0, \vec{P}; \rho)]^{-1} V(\sqrt{s}) \quad (2)$$

which is the solution of Bethe-Salpeter equation(Fig.2), where the kernel matrix V have been factorized on shell as shown in ref.[17] and ref.[18], and G is a diagonal matrix of loop functions. The kernel has nothing to do with nuclear matter and does not depend on density and hence can be parameterized in terms of only the invariant energy \sqrt{s} or $s \equiv (P^0)^2 - \vec{P}^2$. One can find the explicit form of it in ref.[15]. The effects of the nuclear medium are taken into account through the loop functions $G_l(P^0, \vec{P}; \rho)$, which describe the propagation of intermediate states in the medium.

The meson baryon loop functions for the free space are given by the integral

$$G_l(P^0, \vec{P}) = \int \frac{d^4q}{(2\pi)^4} \frac{M_l}{E_l(\vec{P} - \vec{q})} \frac{1}{P^0 - q^0 - E_l(\vec{P} - \vec{q}) + i\epsilon} \frac{1}{(q^0)^2 - \vec{q}^2 - m_l^2 + i\epsilon} \quad (3)$$

which is the zero density limit of the loop function in medium. The generalization to the case where the initial meson baryon system is not in the CM frame ($\vec{P} \neq \vec{0}$), is a necessity in order to evaluate the meson baryon amplitude for arbitrary meson and baryon momenta in the frame of nuclear matter at rest, where the η self-energy is evaluated (see eq.(1)). We regularize the integral by means of a cut off rather than by dimensional regularization as done in ref.[15]. The choice of a cut off is preferable when one performs the calculation in nuclear matter since Lorentz covariance is manifestly broken given the fact that one has a privileged frame of reference, the one where nuclear matter is at rest. The integration variable q is the momentum of the meson in the loop, but in order to obtain a Lorentz invariant quantity when $\rho = 0$ and $\vec{P} \neq 0$, the limits in eq.(3) must be implemented in such a way that the meson momentum in the rest frame of the original meson baryon state, \vec{q}_{cm} , should be smaller than the cut off taken. Another possibility is of course to make a boost and work in the meson baryon CM frame which is the option followed in ref.[14]. Appropriate choices of the cut off and the subtraction constants(a_i) give the equivalent loop functions as in dimensional regularization (see also ref.[19]). Evaluating the integral in CM frame of the meson baryon system, we find that the choice

$$q_{\text{cm}}^{\text{max}} = 1\text{GeV}, \quad a_{\pi N} = 34\text{MeV}, \quad a_{\eta n} = 14\text{MeV}, \quad a_{K\Lambda} = 39\text{MeV}, \quad a_{K\Sigma} = -22\text{MeV} \quad (4)$$

gives meson baryon loop functions equivalent to those in our previous paper. In order to find $G(P^0, \vec{P}; \rho)$ which appears in eq.(2) we shall use the formulation of eq.(3) and eq.(4) in the free case but will take into account Pauli blocking in the intermediate nucleon states, plus the meson and baryon self-energy in the intermediate states.

The Pauli blocking is one of the important nuclear matter effects. We incorporate this by replacing the free nucleon propagator as

$$\frac{1}{P^0 - q^0 - E_l(\vec{P} - \vec{q})} \rightarrow \frac{\theta(|\vec{P} - \vec{q}| - k_F)}{P^0 - q^0 - E_l(\vec{P} - \vec{q})} \quad (5)$$

with the unit step function $\theta(|\vec{P} - \vec{q}| - k_F)$, which prevents the scattering to intermediate nucleon states below the Fermi momentum.

Another important nuclear matter effect is the dressing of hadrons. All the baryons and mesons in the intermediate loops interact with nucleons of the Fermi sea and their dispersion relations are changed. For the baryons, we incorporate this effect, within a mean-field approach, as a momentum-independent binding potential. Due to baryon number conservation, only the difference between the nucleon and hyperon potentials is relevant for our purpose and is introduced in the hyperon propagator in the kaon-hyperon loops. For the mesons, we incorporate the dressing effect by introducing the self-energy function $\Pi_l(q^0, \vec{q}; \rho)$. The meson propagators are replaced, using the Lehmann representation, as

$$\frac{1}{(q^0)^2 - \vec{q}^2 - m_l^2} \rightarrow \frac{1}{(q^0)^2 - \vec{q}^2 - m_l^2 - \Pi_l(q^0, \vec{q}; \rho)} \quad (6)$$

$$= \int_0^\infty d\omega \, 2\omega \frac{S_l(\omega, \vec{q}; \rho)}{(q^0)^2 - \omega^2 + i\epsilon} \quad (7)$$

where $S_l(q^0, \vec{q}; \rho)$ is meson spectral function given by

$$S_l(q^0, \vec{q}; \rho) = -\frac{1}{\pi} \frac{\text{Im}[\Pi_l(q^0, \vec{q}; \rho)]}{|(q^0)^2 - \vec{q}^2 - m_l^2 - \Pi_l(q^0, \vec{q}; \rho)|^2} \quad (8)$$

as a function of energy and momentum in the nuclear matter frame.

Summarizing, the in-medium πN loop function, for example, is calculated by

$$G_{\pi N}(P^0, \vec{P}; \rho) = a_{\pi N} + \int \frac{d^4 q}{(2\pi)^4} \theta(q_{\text{cm}}^{\text{max}} - |\vec{q}_{\text{cm}}|) \frac{M_N}{E_N(\vec{P} - \vec{q})} \frac{\theta(|\vec{P} - \vec{q}| - k_F)}{P^0 - q^0 - E_N(\vec{P} - \vec{q}) + i\epsilon} \int_0^\infty d\omega \frac{2\omega S_\pi(\omega, \vec{q}; \rho)}{(q^0)^2 - \omega^2 + i\epsilon} \quad (9)$$

with

$$\vec{q}_{\text{cm}} = \left[\left(\frac{P^0}{\sqrt{s}} - 1 \right) \frac{\vec{P} \cdot \vec{q}}{|\vec{P}|^2} - \frac{q^0}{\sqrt{s}} \right] \vec{P} + \vec{q} \quad (10)$$

from the Lorentz boost.

The 2-loop function needed for the $\pi\pi N$ channels is also modified in nuclear matter. We still take a zero constant for the real part according to our previous study in the free space [15]. On the other hand, the imaginary part is modified along the lines of $G_{\pi N}$ and we obtain

$$\begin{aligned} \text{Im}[G_{\pi\pi N}(P^0, \vec{P}; \rho)] &= - \int \frac{d^3 \vec{q}_1}{(2\pi)^3} \int \frac{d^3 \vec{q}_2}{(2\pi)^3} (\vec{q}_1 - \vec{q}_2)^2 \frac{M_N}{E_N} \theta(|\vec{P} - \vec{q}_1 - \vec{q}_2| - k_F) \\ &\quad \times \theta(P^0 - E_N) \pi \int_0^\infty d\omega S_\pi(\omega, \vec{q}_1; \rho) S_\pi(P^0 - E_N - \omega, \vec{q}_2; \rho) \end{aligned} \quad (11)$$

with $E_N \equiv E_N(\vec{P} - \vec{q}_1 - \vec{q}_2)$ when both the Pauli blocking and the dressed pion are considered.

3 Input

We use commonly accepted values of baryon binding potentials which are $-70 \rho/\rho_0$ MeV for the nucleon and $-30 \rho/\rho_0$ MeV for the hyperons. Hence, the difference $+40 \rho/\rho_0$ MeV is added to the hyperon energy E_Y in the hyperon propagator.

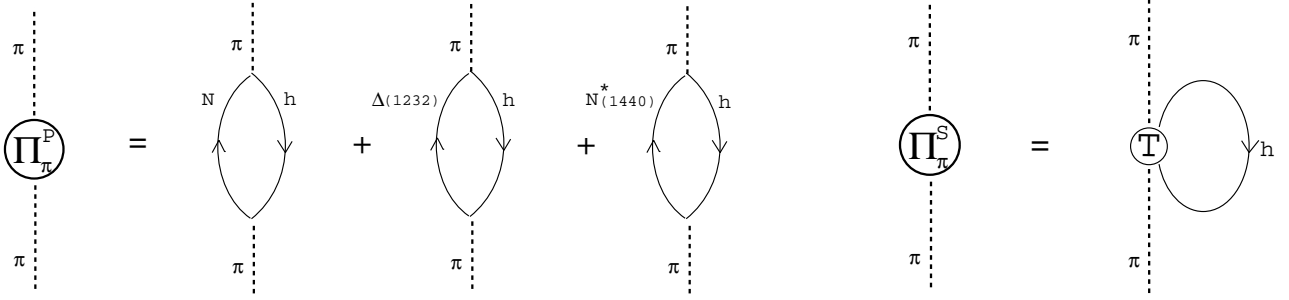


Figure 3: Diagrammatic representation of the P-wave(left) and S-wave(right) term of pion self-energy. The crossed diagrams are omitted in the figure.

The effective K - N interaction in the medium is studied in ref.[20, 21, 17] and the resulting kaon self-energy is $\Pi_K(\rho) = 0.13 m_K^2 \rho/\rho_0$ approximately. We use this real constant self-energy for kaons in the kaon-hyperon loops.

The pion self-energy which we use in the πN and $\pi\pi N$ loops, consists of a P-wave term and an S-wave term as shown in Fig.3. The P-wave term includes N-h, $\Delta(1232)$ -h and $N^*(1440)$ -h excitations, and is basically given by

$$\Pi_\pi^P(q^0, \vec{q}; \rho) = \left(\frac{f_{\pi NN}}{m_\pi} \right)^2 \vec{q}^2 \left\{ U_N(q^0, \vec{q}; \rho) + U_\Delta(q^0, \vec{q}; \rho) + U_{N^*}(q^0, \vec{q}; \rho) \right\} \quad (12)$$

where $f_{\pi\pi N} = 1.02$, and $U_N(q^0, \vec{q}; \rho)$, $U_\Delta(q^0, \vec{q}; \rho)$ and $U_{N^*}(q^0, \vec{q}; \rho)$ are the Lindhard functions corresponding to the above excitations respectively. For example, $U_{N^*}(q^0, \vec{q}; \rho)$ is given by

$$U_{N^*}(q^0, \vec{q}; \rho) = \frac{3}{2} \left(\frac{f_{\pi NN^*}}{f_{\pi NN}} \right)^2 \rho \frac{M_{N^*}}{|\vec{q}|k_F} \left[z + \frac{1}{2}(1 - z^2) \ln \frac{z + 1}{z - 1} + z' + \frac{1}{2}(1 - z'^2) \ln \frac{z' + 1}{z' - 1} \right] \quad (13)$$

$$z = \frac{M_{N^*}}{|\vec{q}|k_F} \left(q^0 - \frac{\vec{q}^2}{2M_{N^*}} - (M_{N^*} - M_N) + \frac{i}{2}\Gamma_{N^*}(q^0, \vec{q}) \right) \quad (14)$$

$$z' = \frac{M_{N^*}}{|\vec{q}|k_F} \left(-q^0 - \frac{\vec{q}^2}{2M_{N^*}} - (M_{N^*} - M_N) + \frac{i}{2}\Gamma_{N^*}(-q^0, \vec{q}) \right) \quad (15)$$

where we use $f_{\pi NN^*}/f_{\pi NN} = 0.477$. This term is small compared to the Δ -h excitation term whose coupling is $f_{\pi N\Delta}/f_{\pi NN} = 2.13$, but has a sizable contribution for energetic pions. The expression for U_Δ is analogous to that in eq.(13-15) and is given in ref.[22], the factor 3/2 in eq.(13) is replaced by 2/3 and the coupling, mass and width of the N^* are replaced by the corresponding magnitudes for the Δ . In the actual calculation we use the P-wave contribution eq.(12) improving with a form factor, a short range correlation and a recoil factor as

$$\left(\frac{f_{\pi NN}}{m_\pi} \right)^2 \vec{q}^2 \sum_i U_i(q^0, \vec{q}; \rho) \rightarrow \left(\frac{f_{\pi NN}}{m_\pi} \right)^2 \vec{q}^2 F(q^0, \vec{q})^2 \sum_i U_i(q^0, \vec{q}; \rho) \quad (16)$$

$$\sum_i U_i(q^0, \vec{q}; \rho) \rightarrow \frac{\sum_i U_i(q^0, \vec{q}; \rho)}{1 - \left(\frac{f_{\pi NN}}{m_\pi} \right)^2 g' \sum_i U_i(q^0, \vec{q}; \rho)} \quad (17)$$

$$U_i(q^0, \vec{q}; \rho) \rightarrow \begin{cases} \left(1 - \frac{q^0}{2M_N} \right)^2 U_N(q^0, \vec{q}; \rho) \\ \left(1 - \frac{q^0}{M_\Delta} \right)^2 U_\Delta(q^0, \vec{q}; \rho) \\ \left(1 - \frac{q^0}{2M_{N^*}} \right)^2 U_{N^*}(q^0, \vec{q}; \rho) \end{cases} \quad (18)$$

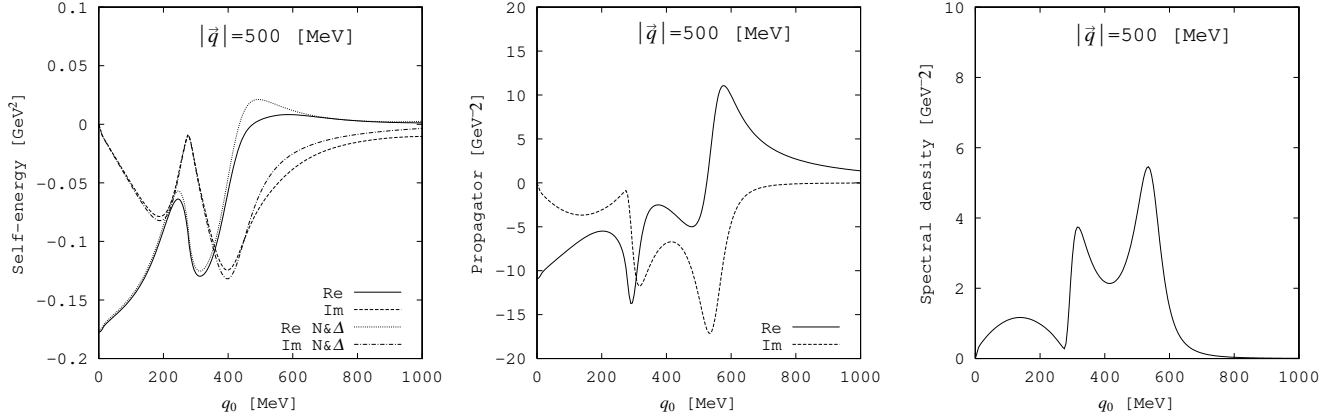


Figure 4: Self-energy(left), propagator(center) and spectral function(right) of a pion for 500 MeV momentum, at normal nuclear matter density. The dotted and dashed dotted lines in the self-energy(left) correspond to the conventional ones including only the N -h and Δ -h excitations.

respectively, where $F(q^0, \vec{q})$ is a monopole form factor with cutoff of 1.2 GeV and $g' = 0.6$.

The S-wave term of the pion self-energy is taken in the so called “ $T\rho$ ” approximation,

$$\Pi_{\pi}^S(q^0, \vec{q}; \rho) = T_{\pi N} \times \rho = \left\{ \frac{1}{3}T_{1/2} + \frac{2}{3}T_{3/2} \right\} \times \rho \quad (19)$$

using the free space S-wave π - N scattering amplitudes calculated in the present model. This term includes the contribution of $N^*(1535)$ -h excitation through the isospin 1/2 amplitude $T_{1/2}$, and is small compared to the P-wave one and becoming only sizable for very energetic pions with about 700 MeV momentum.

The total self-energy of pion is given by $\Pi_{\pi}^P(q^0, \vec{q}; \rho) + \Pi_{\pi}^S(q^0, \vec{q}; \rho)$ and in Fig.4 we show the self-energy(left), propagator(center) and spectral function(right) of the pion for 500 MeV momentum for normal nuclear matter density. In the self-energy(left) graph, the accompanying dotted and dashed dotted lines correspond to the case when we take only the N -h and Δ -h excitations. They show that the contribution of $N^*(1440)$ is relatively small.

One of the needed input in our evaluation is the self-energy of the η which appears in the ηn loop. However, this is not known beforehand since this is what we want to calculate here. We perform for this purpose a self-consistent calculation. In a first step, the $T\rho$ approximation is used since we have previously calculated the free ηn T matrix. With this we obtain a new self-energy of the η which is introduced in the second step, and so on until convergence is reached and one obtains an output η self-energy equal to the input one.

4 Results

Fig.5 shows the free space η -neutron scattering amplitude $T_{\eta n}$ obtained in the present model. It is plotted as a function of the invariant energy \sqrt{s} , which is 1487 MeV at the threshold. One sees that the amplitude changes drastically, even from attractive to repulsive, above the threshold. This is due to the coupling to the $N^*(1535)$ resonance which is generated dynamically in the present model. Note that the threshold is about 50 MeV below the center of the resonance. We can obtain the η self-energy as an explicit function of k^0 and \vec{k} as independent variables. One of the interesting applications is the study of η bound states in the nucleus, where the η will

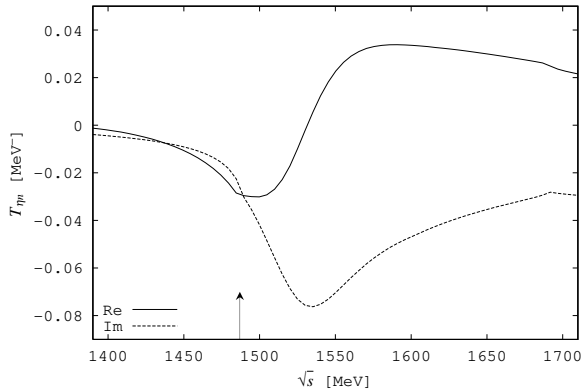


Figure 5: The free space $T_{\eta n}$ amplitude as a function of the invariant energy \sqrt{s} . The arrow shows the ηn threshold.

have small energy and momenta. For this purpose we can evaluate the η self-energy for $k^0 = m_\eta$ and $\vec{k} = 0$ as a good approximation. Non-local effects from the consideration of the energy and momentum dependence of the self-energy give very small corrections for weakly bound states as demonstrated in ref.[23] for K^- atoms.

In order to evaluate the η self-energy in a first step, we substitute the free ηn amplitude in eq.(1), setting $\vec{k} = \vec{0}$, and obtain the η self-energy for zero momentum shown in Fig.6 top. This simplest calculation is nearly equal to the $T\rho$ approximation. The magnitude of the self-energy increases almost linearly in ρ and its shape reflects that of $T_{\eta n}$.

Then we turn on the Pauli blocking in the way explained in section 2. The resulting η self-energy for zero momentum is shown in Fig.6 middle. Comparing to the top one, we see the interesting effects of the Pauli blocking. First of all, the resonant shape is strongly enhanced. This can be understood as the reduction of the decay width of the resonance, since the Pauli blocking forbids the decay to nucleons with momentum smaller than k_F . Second, the peak of the resonance, seen in the imaginary part of the amplitudes, or equivalently in the zero of the real part, is only shifted moderately to higher energies. This is in contrast with the \bar{K} case, where the $\Lambda(1405)$ resonance in the $\bar{K}N$ interaction, is about 80 MeV shifted upward [24, 14]. As pointed out in ref.[24], this is natural because a large part of the $N^*(1535)$ resonance generated in the present model, comes from the $K^+\Sigma$, $K^0\Sigma^0$ and $K^0\Lambda$ components [25, 21, 15], which have nothing to do with Pauli blocking. In ref.[24] it is argued that the Fermi motion compensates the decay width reduction due to the Pauli blocking. There also is some effect of this sort here, but we still find a net reduction of the $N^*(1535)$ width due to the consideration of both effects, resulting in an enhanced strength of both the real and imaginary parts of the η self-energy. A major difference in our model from ref.[24], at the present stage of the calculation, is the presence of the 3-body $\pi\pi N$ channels. Also, our free space $T_{\eta n}(\sqrt{s})$ shown in Fig.5, is already different from that in ref.[24], where the peak of the resonance is seen at around 1590 MeV.

Finally, we turn on the dressing of the hadrons in addition to Pauli blocking. This study is the main novelty of the present work. We use the input explained in the previous section. Besides this, we need the spectral function of the η in order to calculate the ηn loop function. As stated in the previous section, we determine it in a self-consistent way by iterating the Bethe-Salpeter equation. This means that we need to study the finite momentum case even if we are interested only in the η with zero momentum. We, hence, evaluate the η self-energy also for finite momentum and, for example, Fig.7 left shows a rough sketch of the η spectral function obtained at normal

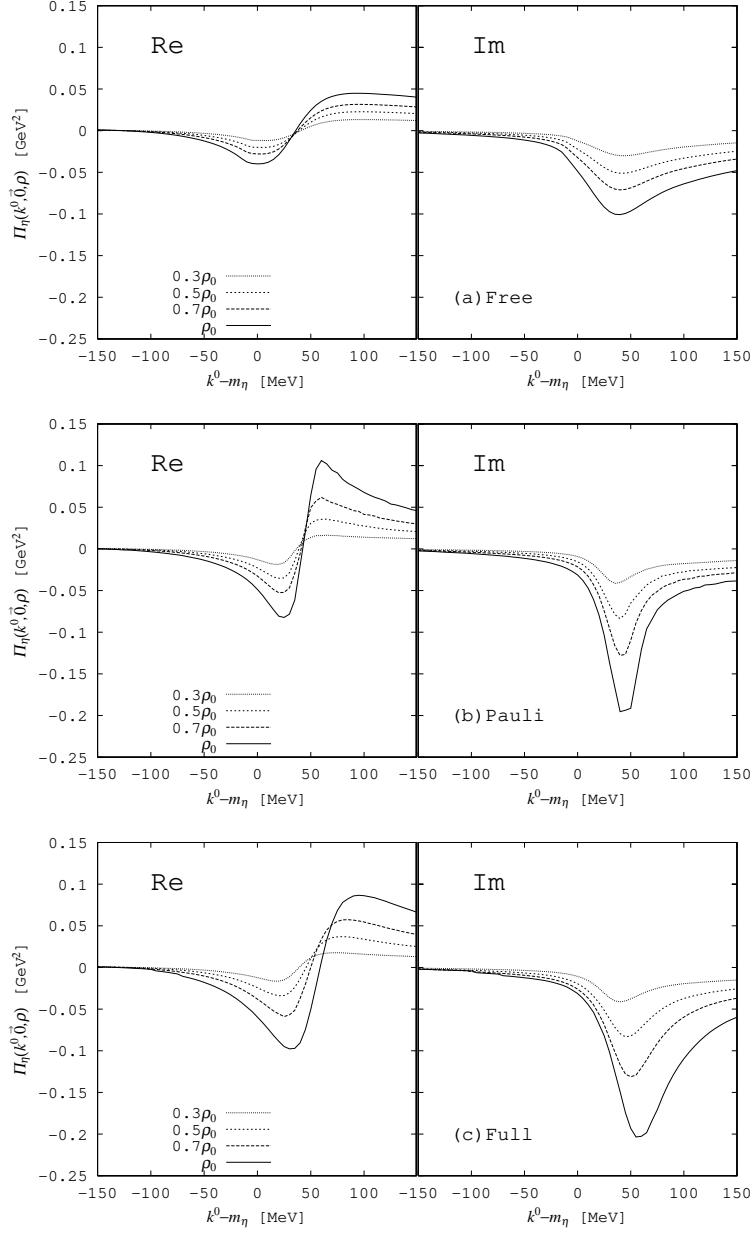


Figure 6: η self-energy for zero momentum as a function of energy, for four different densities and in three different approximations. Top, (a) Free: the free space η - N amplitude is used. Middle, (b) Pauli: the Pauli blocking is taken into account. Bottom, (c) Full: both the Pauli blocking and hadron dressing are taken into account.

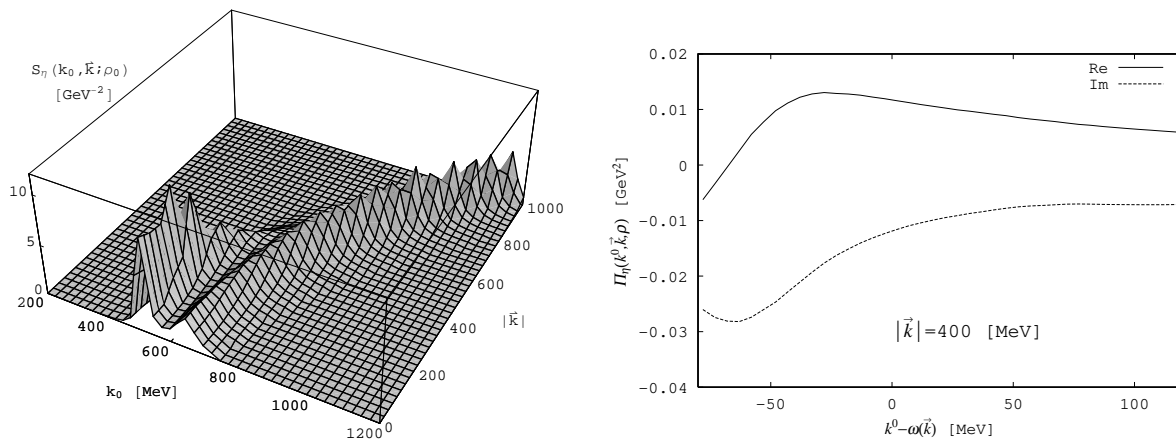


Figure 7: Left: A rough sketch of the η spectral function at normal nuclear matter density, where the peak value is not realistic because of the plotting resolution. Right: Self-energy of the η with 400 MeV momentum at normal nuclear matter density as a function of energy.

nuclear matter density as a function of k^0 and \vec{k} . The results in what follows include the dressed η accounting for the η self-energy as a function k^0 and \vec{k} .

The η self-energy for zero momentum obtained in this self-consistent approach is shown in Fig.6 bottom. One can see the effects of the hadron dressing in comparison to the middle figure of the panel. Apparently, the strength is spread wider. This is expected because the η spectrum is distributed as stated above. Even then, the resonant shape is still clearly visible. The center of the resonance is shifted upward, for example, about 25 MeV for normal nuclear matter density. This means that the sum of the repulsion on K and so on, surpasses the attraction on the pions. The difference of the hyperon binding energy and the nucleon one, works as a repulsion for this calculation. The dressed η also shifts it upward slightly because the η with large momentum (larger than about 250 MeV) feels a weak repulsion, as shown in Fig.7 right. Recall that the $K\Sigma$, $K\Lambda$ and ηn components are more important than the πN and $\pi\pi N$ components for the resonance in the present model. The 25 MeV shift for normal nuclear matter density is small (less than 2% of the $N^*(1535)$ mass) and consistent with η photo-production data [26], which together with the theoretical analysis of ref.[27] assuming no shift of the resonance, suggest that the in-medium mass of the resonance is almost the same as in free space.

Fig.8 left shows the spectral function of a zero momentum η corresponding to the final self-energy. We see still a narrow peak even for normal nuclear matter density and, hence, it makes sense to regard the η in the medium as a quasi-particle with a modified mass. It is interesting to note a second peak in the spectral function at higher energies, which, as noted in ref.[24], comes from the coupling of the η to the $N^*(1535)$ -h. We can observe in the figure that as the density increases the two peaks move away from each other.

We define the effective mass $m_\eta^*(\rho)$ as the energy k^0 which satisfies

$$(k^0)^2 - m_\eta^2 - \text{Re}[\Pi_\eta(k^0, \vec{0}; \rho)] = 0, \quad (20)$$

which is almost the position of the peak in the spectral function. The result is plotted in Fig.8 right, which indicates that approximately one has

$$\frac{m_\eta^*}{m_\eta} \simeq 1 - 0.05 \frac{\rho}{\rho_0} \quad (21)$$

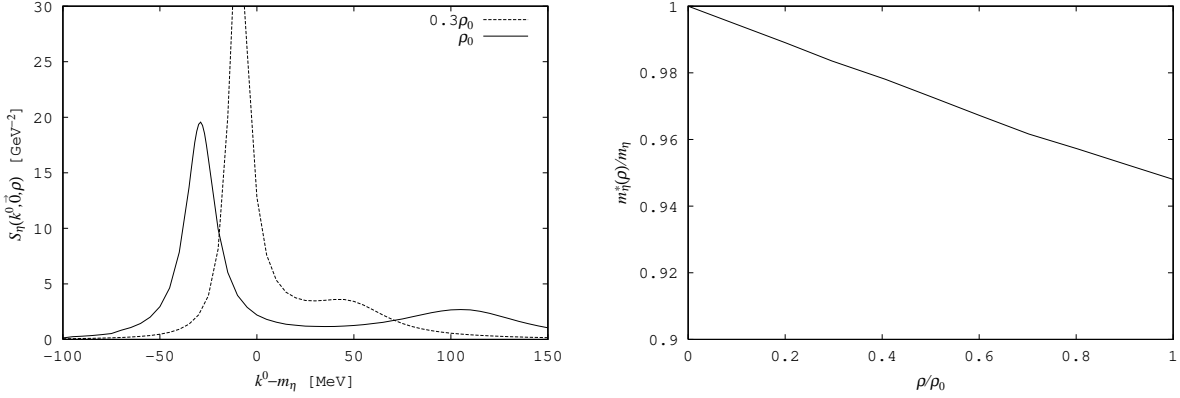


Figure 8: Left: η spectral density for the zero momentum. Right: Effective mass of the η as a function of density.

in short. This moderate downward shift agree with the result of [24]. While, a much stronger, about 11%, downward shift for normal nuclear matter density, is reported in [28] where the quark meson coupling model is used. It should be interesting to test these predictions from experimental data of η mesic nuclei.

The optical potential $U_\eta(\rho)$ and the effective η -neutron scattering length $a_{\eta n}^*(\rho)$ defined as

$$U_\eta(\rho) = \frac{\Pi_\eta(m_\eta, \vec{0}, \rho)}{2m_\eta} \quad (22)$$

$$a_{\eta n}^*(\rho) = -\frac{1}{4\pi} \frac{M_n}{M_n + m_\eta} \frac{\Pi_\eta(m_\eta, \vec{0}, \rho)}{\rho} \quad (23)$$

are useful when we study the bound state of an η in nuclei using the local density approximation. We plot them in Fig.9. One can see that the real and imaginary parts of the optical potential deviate as the density increases. The real part becomes larger than the linear $T\rho$ approximation while the imaginary part is nearly $T\rho$. This behavior is better seen in the effective scattering length, where the real part increases and the imaginary part almost stays the same. The depth of the optical potential at normal nuclear matter density is $-54 - i29$ MeV. This value is not in contradiction with the 5% (28 MeV) mass shift of the η , because the self-energy is evaluated at an η energy equal to the η mass, while the effective η mass, k^0 in eq.(20), is obtained using the η self-energy calculated at same k^0 energy. It is interesting to compare these result with the ones obtained in the literature. In ref.[24] the potential obtained was $U_\eta(\rho) \simeq (-20 - i22) \rho/\rho_0$ MeV which provides an imaginary part similar to ours but the real part is about one half of the one obtained here. In ref.[29] the potential obtained assuming that the mass of the $N^*(1535)$ did not change in the medium, as we showed it was approximately the case here, was $U_\eta(\rho) = (-34 - i24)$ MeV at $\rho = \rho_0$, somewhere in between the two former results.

In order to facilitate the task of making an accurate as possible prediction for the η bound states in nuclei, we parameterize our results for the η self-energy as a function of energy and density. Given the strong energy dependence of the $\Pi_\eta(k^0, \vec{0}; \rho)$ seen in Fig.6 for $k^0 - m_\eta < 0$, the consideration of this explicit energy dependence in the Klein-Gordon equation should be important. We can parameterize our results in the region $-50 \text{ MeV} < k^0 - m_\eta < 0$, as

$$\text{Re}[\Pi_\eta(k^0, \vec{0}; \rho)] = a(\rho) + b(\rho)(k^0 - m_\eta) + c(\rho)(k^0 - m_\eta)^2 + d(\rho)(k^0 - m_\eta)^3 \quad (24)$$

$$\text{Im}[\Pi_\eta(k^0, \vec{0}; \rho)] = e(\rho) + f(\rho)(k^0 - m_\eta) + g(\rho)(k^0 - m_\eta)^2 + h(\rho)(k^0 - m_\eta)^3 \quad (25)$$

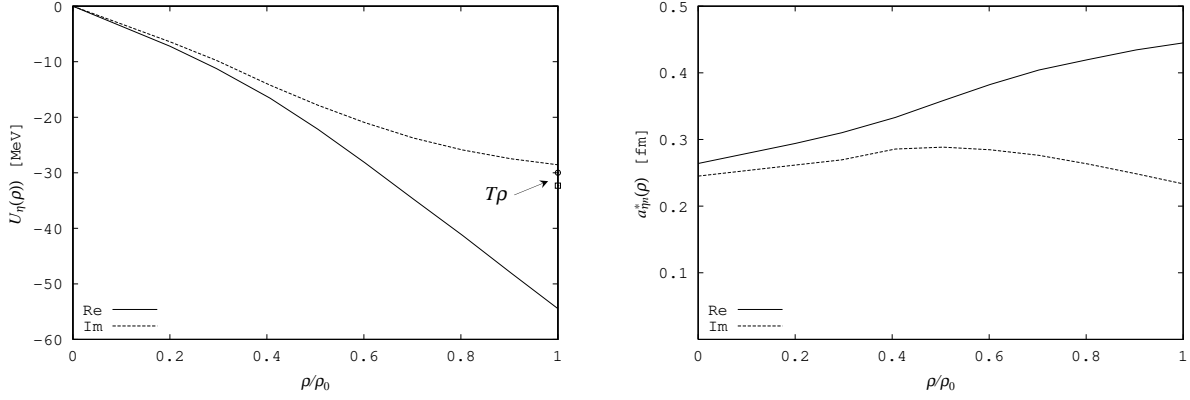


Figure 9: Left: η optical potential as a function of density. The box and circle stand for the real and imaginary parts of the potential in the $T\rho$ approximation with the threshold $T_{\eta m}$ corresponding to a scattering length of $0.26 + i0.24$ fm [15]. Right: η - n effective scattering length as a function of density.

with

$$a(\rho) = -36200.3 \rho/\rho_0 - 24166.6 \rho^2/\rho_0^2 \text{ MeV}^2 \quad (26)$$

$$b(\rho) = -1060.05 \rho/\rho_0 - 326.803 \rho^2/\rho_0^2 \text{ MeV} \quad (27)$$

$$c(\rho) = -13.2403 \rho/\rho_0 - 0.154177 \rho^2/\rho_0^2 \quad (28)$$

$$d(\rho) = -0.0701901 \rho/\rho_0 + 0.0173533 \rho^2/\rho_0^2 \text{ MeV}^{-1} \quad (29)$$

$$e(\rho) = -43620.9 \rho/\rho_0 + 11408.4 \rho^2/\rho_0^2 \text{ MeV}^2 \quad (30)$$

$$f(\rho) = -1441.14 \rho/\rho_0 + 511.247 \rho^2/\rho_0^2 \text{ MeV} \quad (31)$$

$$g(\rho) = -27.6865 \rho/\rho_0 + 10.0433 \rho^2/\rho_0^2 \quad (32)$$

$$h(\rho) = -0.221282 \rho/\rho_0 + 0.0840531 \rho^2/\rho_0^2 \text{ MeV}^{-1} \quad (33)$$

By using the Klein-Gordon equation, and substituting $\rho \rightarrow \rho(r)$ in the spirit of the local density approximation, one can then obtain binding energies and widths of the η state in different nuclei.

5 Conclusion

In the present paper we have used a chiral unitary approach successfully applied to the study of the πN interaction and its coupled channels, in particular the ηN channel, in order to evaluate the η self-energy in a nuclear medium. We have taken into account the standard many body effects like Fermi motion and the Pauli blocking in the intermediate N states. In addition we have also included the self-energy of the baryons and mesons in the intermediate states, including the η self-energy in a self-consistent way. The results obtained are interesting. While qualitatively similar to other ones obtained before, we obtain however a deeper potential with a real part about twice as big as in former, more simplified, studies. In addition we show that the energy dependence of the η self-energy is very pronounced below the η threshold and it would be interesting to consider it in studies of η bound states in nuclei. For this purpose we have parameterized our results in an easy analytical form which can be used to solve the Klein-Gordon equation for η bound states or to interpret some physical processes where η states close to threshold play some role [30]. The stronger real part of our potential compared to previous ones and the fact that the imaginary part

of the potential decreases rapidly as the η energy decreases, open new hopes that η mesic states, relatively wide, but narrow enough compared to the binding energy, could exist and be identified in actual experiments.

Acknowledgments

We would like to thank Prof. M.J. Vicente Vacas for useful discussions. This work has been partly supported by the Spanish Ministry of Education in the program “Estancias de Doctores y Tecnólogos Extranjeros en España”, by the DGICYT contract number BFM2000-1326 and by the EU TMR network Eurodaphne, contact no. ERBFMRX-CT98-0169.

References

- [1] CERES Collaboration, G. Agakishiev et al., Phys. Rev. Lett. 75(1995)1272
- [2] CERES Collaboration, B. Lenkeit et al., Nucl. Phys. A661(1999)23
- [3] CERES/NA45 Collaboration, K. Filimonov et al., nucl-ex/0109017
- [4] DLS Collaboration, R.J. Porter et al., Phys. Rev. Lett. 79(1997)1229
- [5] E325 Collaboration, K. Ozawa et al., Phys. Rev. Lett. 86(2001)5019
- [6] HADES Collaboration, J.Friese, Prog. Part. Nucl. Phys. 42(1999)235
- [7] E.L. Bratkovskaya, W. Cassing, U.Mosel, Nucl. Phys. A686(2001)568
- [8] T. Yamazaki et al., Z. Phys. A355(1996)219; T. Yamazaki et al., Phys Lett. B418(1998)246; H. Gilg et al., Phys. Rev. C62(2000)025201; K. Itahashi et al. Phys Rev. C62(2000)025202
- [9] H. Geissel et al., Nucl. Phys. A663(200)206c
- [10] M. Ericson and T.F.O. Ericson, Ann. Phys. 36(1966)323
- [11] J. Nieves, E. Oset and C. Garcia Recio, Nucl. Phys. A554(1993)509
- [12] C.J. Batty, E.Friedman and A. Gal, Phys. Rept. 287(1997)385
- [13] R.S. Hayano, S. Hirenzaki and A. Gillitzer, Eur. Phys. J. A6(1999)105
- [14] A. Ramos and E. Oset, Nucl. Phys. A671(2000)481
- [15] T. Inoue, E. Oset and M. J. Vicente Vacas, Phys. Rev C 65(2002)035204
- [16] J. Nieves and E. Ruiz Arriola, Phys. Rev D64(2001)116008
- [17] E. Oset and A. Ramos, Nucl. Phys. A635(1998)99
- [18] J.A. Oller and U.G. Meissner, Phys. Lett. B500(2001)263
- [19] E. Oset, A. Ramos and C. Bennhold, Phys. Lett. B522(2002)260

- [20] N. Kaiser, P.B. Siegel and W. Weise, Nucl. Phys. A594(1995)325
- [21] N. Kaiser, T. Waas and W. Weise, Nucl. Phys. A 612(1997)297
- [22] E. Oset, P. Fernandez de Cordoba, L.L. Salcedo and R. Brockmann, Phys. Rept. 188(1990)79
- [23] C. Garcia-Recio, J. Nieves, E. Oset and A. Ramos, Nucl. Phys. A in print, nucl-th/0012075
- [24] T. Waas and W.Weise, Nucl. Phys. A625(1997)287
- [25] N. Kaiser, P.B. Siegel and W. Weise, Phys. Lett. B362(1995)23
- [26] M. Röbig-Landau et. al., Phys. Lett. B373(1996)45
- [27] R.C. Carrasco, Phys. Rev. C48(1993)2333
- [28] K. Tsushima, D.H. Lu and A.W. Thomas, Phys. Lett. B443(1998)26
- [29] H.C. Chiang, E. Oset and L.C. Liu, Phys. Rev. C44(1991)738
- [30] K.P. Khemchandani, N.G. Kelkar and B.K. Jain, nucl-th/0112065